

# Study of a possibility of observation of hidden-bottom pentaquark resonances in bottomonium photoproduction on protons and nuclei near threshold

E. Ya. Paryev<sup>1,2</sup>

<sup>1</sup>*Institute for Nuclear Research, Russian Academy of Sciences,  
Moscow 117312, Russia*

<sup>2</sup>*Institute for Theoretical and Experimental Physics,  
Moscow 117218, Russia*

## Abstract

We study the  $\Upsilon(1S)$  meson photoproduction on protons and nuclei at the near-threshold center-of-mass energies below 11.4 GeV (or at the corresponding photon laboratory energies  $E_\gamma$  below 68.8 GeV). We calculate the absolute excitation functions for the non-resonant and resonant photoproduction of  $\Upsilon(1S)$  mesons off protons at incident photon laboratory energies of 63–68 GeV by accounting for direct ( $\gamma p \rightarrow \Upsilon(1S)p$ ) and two-step ( $\gamma p \rightarrow P_b^+(11080, 11125, 11130) \rightarrow \Upsilon(1S)p$ )  $\Upsilon(1S)$  production channels within different scenarios for the non-resonant total cross section of elementary reaction  $\gamma p \rightarrow \Upsilon(1S)p$  and for branching ratios of the decays  $P_b^+(11080, 11125, 11130) \rightarrow \Upsilon(1S)p$ . We also calculate analogous functions for photoproduction of  $\Upsilon(1S)$  mesons on  $^{12}\text{C}$  and  $^{208}\text{Pb}$  target nuclei in the near-threshold center-of-mass beam energy region of 9.0–11.4 GeV by considering respective incoherent direct ( $\gamma N \rightarrow \Upsilon(1S)N$ ) and two-step ( $\gamma p \rightarrow P_b^+(11080, 11125, 11130) \rightarrow \Upsilon(1S)p$ ,  $\gamma n \rightarrow P_b^0(11080, 11125, 11130) \rightarrow \Upsilon(1S)n$ )  $\Upsilon(1S)$  production processes within a nuclear spectral function approach. We show that a detailed scan of the  $\Upsilon(1S)$  total photoproduction cross section on a proton and nuclear targets in the near-threshold energy region in future high-precision experiments at the proposed high-luminosity electron-ion colliders EIC and EicC in the U.S. and China should give a definite result for or against the existence of the non-strange hidden-bottom pentaquark states  $P_{bi}^+$  and  $P_{bi}^0$  ( $i=1, 2, 3$ ) as well as clarify their decay rates.

# 1. Introduction

In a recent publication [1] the role of the new narrow hidden-charm pentaquark states  $P_c^+(4312)$ ,  $P_c^+(4440)$  and  $P_c^+(4457)$ , discovered by the LHCb Collaboration in  $J/\psi p$  invariant mass spectrum of the  $\Lambda_b^0 \rightarrow K^-(J/\psi p)$  decays [2], in near-threshold  $J/\psi$  photoproduction on nuclei has been studied in the framework of the nuclear spectral function approach by considering both the direct non-resonant ( $\gamma N \rightarrow J/\psi N$ ) and the two-step resonant ( $\gamma p \rightarrow P_c^+(4312)$ ,  $P_c^+(4312) \rightarrow J/\psi p$ ;  $\gamma p \rightarrow P_c^+(4440)$ ,  $P_c^+(4440) \rightarrow J/\psi p$  and  $\gamma p \rightarrow P_c^+(4457)$ ,  $P_c^+(4457) \rightarrow J/\psi p$ )  $J/\psi$  elementary production processes<sup>1)</sup>. In the calculations the new experimental data for the total and differential cross sections of the exclusive reaction  $\gamma p \rightarrow J/\psi p$  in the threshold energy region from the GlueX experiment [5] have been incorporated. The model-dependent upper limits on branching ratios of  $P_c^+(4312) \rightarrow J/\psi p$ ,  $P_c^+(4440) \rightarrow J/\psi p$  and  $P_c^+(4457) \rightarrow J/\psi p$  decays, set in this experiment, have been accounted for in them as well.

The quark structure of the above pentaquarks is  $|P_c^+ \rangle = |uudc\bar{c} \rangle$ , i.e., they are composed of three light quarks  $u, u, d$  and a charm-anticharm pair  $c\bar{c}$ . In a molecular scenario, due to the closeness of the observed  $P_c^+(4312)$  and  $P_c^+(4440)$ ,  $P_c^+(4457)$  masses to the  $\Sigma_c^+ \bar{D}^0$  and  $\Sigma_c^+ \bar{D}^{*0}$  thresholds, the  $P_c^+(4312)$  resonance can be, in particular, considered as an S-wave  $\Sigma_c^+ \bar{D}^0$  bound state, while the  $P_c^+(4440)$  and  $P_c^+(4457)$  as S-wave  $\Sigma_c^+ \bar{D}^{*0}$  bound molecular states [6–18]. The existence of molecular type hidden-charm pentaquark resonances has been predicted before the LHCb observation [2, 3] in some earlier papers (see, for example, [19]). It is natural to extend this picture to the bottom sector replacing the  $c\bar{c}$  pair on the bottom-antibottom  $b\bar{b}$  pair as well as the non-strange  $D(D^*)$  mesons on  $B(B^*)$  ones and the charmed baryons by the bottom ones. Based on the classification of hidden-charm pentaquarks composed by a single charm baryon and  $D(D^*)$  mesons, such extension has been performed in Ref. [20] within the hadronic molecular approach. As a result, the classification of hidden-bottom pentaquarks composed by a single bottom baryon and  $B(B^*)$  mesons has been presented here. According to it, the charged hidden-bottom partners  $P_b^+(11080)$ ,  $P_b^+(11125)$  and  $P_b^+(11130)$  of the observed hidden-charm pentaquarks  $P_c^+(4312)$ ,  $P_c^+(4440)$  and  $P_c^+(4457)$ , having the quark structure  $|P_b^+ \rangle = |uudb\bar{b} \rangle$ , were predicted to exist, with masses of 11080, 11125 and 11130 MeV, respectively. Moreover, the predictions for the neutral hidden-bottom counterparts  $P_b^0(11080)$ ,  $P_b^0(11125)$  and  $P_b^0(11130)$  of the unobserved hidden-charm states  $P_c^0(4312)$ ,  $P_c^0(4440)$  and  $P_c^0(4457)$  with the quark structure  $|P_b^0 \rangle = |uddb\bar{b} \rangle$  were provided in [20] as well. These new exotic heavy pentaquarks can decay into the  $\Upsilon(1S)p$  and  $\Upsilon(1S)n$  final states, correspondingly. They can be searched for through a scan of the cross section<sup>2)</sup> of the exclusive reaction  $\gamma p \rightarrow \Upsilon(1S)p$  from threshold of 10.4 GeV and up to photon  $\gamma p$  c.m.s. energy  $W = 11.4$  GeV (cf. [21]).

Therefore, it is interesting to extend the study of Ref. [1] to the consideration of bottomonium  $\Upsilon(1S)$  photoproduction on protons and nuclei near threshold to shed light on the possibility to observe such hidden-bottom pentaquarks in this photoproduction in future high-precision experiments at the proposed high-luminosity electron-ion colliders EIC [22–24] and EicC [25, 26] in the U.S. and China. This is the main purpose of the present paper. We briefly remind the main assumptions of the model [1] and describe, where it is necessary, the corresponding extensions. We present also the predictions obtained within this expanded model for the  $\Upsilon(1S)$  excitation functions in  $\gamma p$  as well as in  $\gamma^{12}\text{C}$  and  $\gamma^{208}\text{Pb}$  collisions at near-threshold incident energies. They could serve as a guidance for future dedicated experiments at the above colliders.

<sup>1)</sup>It should be noted that such role of initially claimed [3] by the LHCb Collaboration pentaquark resonance  $P_c^+(4450)$  in  $J/\psi$  photoproduction on nuclei at near-threshold incident photon energies of 5–11 GeV has been investigated in our previous work [4].

<sup>2)</sup>They should appear as structures at  $W = 11080, 11125$  and  $11130$  MeV or at laboratory photon energies  $E_\gamma = 64.952, 65.484$  and  $65.544$  GeV in this cross section.

## 2. The model

### 2.1. Direct processes of non-resonant $\Upsilon(1S)$ photoproduction on nuclei

An incident photon can produce a  $\Upsilon(1S)$  meson directly in the first inelastic  $\gamma N$  collision. Since we are interested in near-threshold center-of-mass photon beam energies  $\sqrt{s}$  below 11.4 GeV, corresponding to the laboratory incident photon energies  $E_\gamma$  below 68.8 GeV or excess energies  $\epsilon_{\Upsilon(1S)N}$  above the  $\Upsilon(1S)N$  threshold  $\sqrt{s_{\text{th}}} = m_{\Upsilon(1S)} + m_N = 10.4$  GeV ( $m_{\Upsilon(1S)}$  and  $m_N$  are the lowest-lying bottomonium and nucleon bare masses, respectively),  $\epsilon_{\Upsilon(1S)N} = \sqrt{s} - \sqrt{s_{\text{th}}} \leq 1.0$  GeV, we have taken into account the following direct non-resonant elementary  $\Upsilon(1S)$  production processes which have the lowest free production threshold <sup>3)</sup> :

$$\gamma + p \rightarrow \Upsilon(1S) + p, \quad (1)$$

$$\gamma + n \rightarrow \Upsilon(1S) + n. \quad (2)$$

In what follows, in line with [27] we will neglect the modification of the outgoing  $\Upsilon(1S)$  mass in nuclear matter. Also, we will ignore the medium modification of the secondary high-momentum nucleon mass in the present work.

Disregarding the absorption of incident photons in the energy range of interest to us and describing the  $\Upsilon(1S)$  meson absorption in nuclear medium by the absorption cross section  $\sigma_{\Upsilon(1S)N}$ , we can represent the total cross section for the production of  $\Upsilon(1S)$  mesons off nuclei in the direct non-resonant channels (1) and (2) of their production off target nucleons in the form [4]:

$$\sigma_{\gamma A \rightarrow \Upsilon(1S)X}^{(\text{dir})}(E_\gamma) = I_V[A, \sigma_{\Upsilon(1S)N}] \left\langle \sigma_{\gamma p \rightarrow \Upsilon(1S)p}(E_\gamma) \right\rangle_A, \quad (3)$$

where

$$I_V[A, \sigma] = 2\pi A \int_0^R r_\perp dr_\perp \int_{-\sqrt{R^2 - r_\perp^2}}^{\sqrt{R^2 - r_\perp^2}} dz \rho(\sqrt{r_\perp^2 + z^2}) \quad (4)$$

$$\times \exp \left[ -A\sigma \int_z^{\sqrt{R^2 - r_\perp^2}} \rho(\sqrt{r_\perp^2 + x^2}) dx \right],$$

$$\left\langle \sigma_{\gamma p \rightarrow \Upsilon(1S)p}(E_\gamma) \right\rangle_A = \int \int P_A(\mathbf{p}_t, E) d\mathbf{p}_t dE \sigma_{\gamma p \rightarrow \Upsilon(1S)p}(\sqrt{s_{\Upsilon(1S)}}) \quad (5)$$

and

$$s_{\Upsilon(1S)} = (E_\gamma + E_t)^2 - (\mathbf{p}_\gamma + \mathbf{p}_t)^2, \quad (6)$$

$$E_t = M_A - \sqrt{(-\mathbf{p}_t)^2 + (M_A - m_N + E)^2}. \quad (7)$$

Here,  $\sigma_{\gamma p \rightarrow \Upsilon(1S)p}(\sqrt{s_{\Upsilon(1S)}})$  is the "in-medium" total cross section for the production of  $\Upsilon(1S)$  in reaction (1) <sup>4)</sup> at the "in-medium"  $\gamma p$  center-of-mass energy  $\sqrt{s_{\Upsilon(1S)}}$ ;  $\rho(\mathbf{r})$  and  $P_A(\mathbf{p}_t, E)$  are the local nucleon density and the nuclear spectral function of target nucleus  $A$  normalized to unity <sup>5)</sup>;  $\mathbf{p}_t$  and  $E$  are the internal momentum and binding energy of the struck target nucleon just before the collision;  $A$  is the number of nucleons in the target nucleus,  $M_A$  and  $R$  are its mass and radius;

<sup>3)</sup>We can ignore in the energy domain of our interest the contribution to the  $\Upsilon(1S)$  yield from the excited bottomonium states  $\Upsilon(2S)$ ,  $\Upsilon(3S)$  and  $\chi_b(1P)$ ,  $\chi_b(2P)$  mesons feed-down due to larger their production thresholds in  $\gamma N$  collisions.

<sup>4)</sup>In equation (3) it is supposed that the  $\Upsilon(1S)$  meson production cross sections in  $\gamma p$  and  $\gamma n$  interactions are the same.

<sup>5)</sup>The concrete information about these quantities, used in our subsequent calculations, is given in [28–30].

$\mathbf{p}_\gamma$  and  $E_\gamma$  are the laboratory momentum and energy of the initial photon. Motivated by the fact that the nuclear medium suppresses  $\Upsilon(1S)$  production as much as  $J/\psi$  production, we will employ for the  $\Upsilon(1S)$ –nucleon absorption cross section  $\sigma_{\Upsilon(1S)N}$  in our calculations the same value of 3.5 mb as was adopted in Ref. [4] for the  $J/\psi$ –nucleon absorption cross section  $\sigma_{J/\psi N}$  (cf. [31–33]).

As earlier in [4], we suggest that the "in-medium" cross section  $\sigma_{\gamma p \rightarrow \Upsilon(1S)p}(\sqrt{s_{\Upsilon(1S)}})$  for  $\Upsilon(1S)$  production in process (1) is equivalent to the vacuum cross section  $\sigma_{\gamma p \rightarrow \Upsilon(1S)p}(\sqrt{s})$  in which the vacuum center-of-mass energy squared  $s$ , presented by the formula

$$s = W^2 = (E_\gamma + m_N)^2 - \mathbf{p}_\gamma^2, \quad (8)$$

is replaced by the in-medium expression (6). The latter cross section has been determined experimentally both earlier [34–36] and recently [37, 38] only at high photon–proton center-of-mass energies  $W = \sqrt{s} > 60$  GeV (see Fig. 2 given below). And up to now, the experimental data on  $\Upsilon(1S)$  production in the channel  $\gamma p \rightarrow \Upsilon(1S)p$  are not available in the threshold energy region  $W \leq 11.4$  GeV, where the masses of the predicted [20]  $P_b$  states are concentrated and where they can be observed [21] in  $\gamma p$  reactions.

The total cross section of this channel can be evaluated using the following indirect route. An analysis of the data on the production of  $\Upsilon(1S)$  and  $J/\psi$  mesons in  $\gamma p$  collisions in the kinematic range of  $80 < W < 160$  GeV, taken by the ZEUS Collaboration at HERA [34], gave the following ratio of the  $\Upsilon(1S)$  to  $J/\psi$  photoproduction cross sections in this range:

$$\sigma_{\gamma p \rightarrow \Upsilon(1S)p}(W) / \sigma_{\gamma p \rightarrow J/\psi p}(W) \approx 5 \cdot 10^{-3}. \quad (9)$$

Accounting for the commonality in the  $J/\psi$  and  $\Upsilon(1S)$  production in  $\gamma p$  interactions [39], we assume that in the threshold region  $W \leq 11.4$  GeV the ratio of the total cross sections of the reactions  $\gamma p \rightarrow \Upsilon(1S)p$  and  $\gamma p \rightarrow J/\psi p$  is the same as that of Eq. (9) derived at the same high  $\gamma p$  c.m.s. energies. But now, in this ratio the former and latter cross sections are calculated, respectively, at the collisional energies  $\sqrt{s}$  and  $\sqrt{\tilde{s}}$  which correspond to the same excess energies  $\epsilon_{\Upsilon(1S)N}$  and  $\epsilon_{J/\psi N}$  above the  $\Upsilon(1S)N$  and  $J/\psi N$  thresholds, viz.:

$$\sigma_{\gamma p \rightarrow \Upsilon(1S)p}(\sqrt{s}) / \sigma_{\gamma p \rightarrow J/\psi p}(\sqrt{\tilde{s}}) \approx 5 \cdot 10^{-3}, \quad (10)$$

where, according to above-mentioned, the center-of-mass energies  $\sqrt{s}$  and  $\sqrt{\tilde{s}}$  are linked by the relation:

$$\epsilon_{J/\psi N} = \sqrt{\tilde{s}} - \sqrt{\tilde{s}_{\text{th}}} = \epsilon_{\Upsilon(1S)N} = \sqrt{s} - \sqrt{s_{\text{th}}}. \quad (11)$$

Here,  $\sqrt{\tilde{s}_{\text{th}}} = m_{J/\psi} + m_N$  ( $m_{J/\psi}$  is the bare  $J/\psi$  meson mass). With this, we have:

$$\sqrt{\tilde{s}} = \sqrt{s} - \sqrt{s_{\text{th}}} + \sqrt{\tilde{s}_{\text{th}}} = \sqrt{s} - m_{\Upsilon(1S)} + m_{J/\psi}. \quad (12)$$

Evidently, that at high energies such that  $\sqrt{s} \gg \sqrt{s_{\text{th}}}$ ,  $\sqrt{\tilde{s}} \approx \sqrt{s}$  and the expression (10) transforms to (9). At low incident photon energies  $\sqrt{s} \leq 11.4$  GeV of interest, the c.m.s. energy  $\sqrt{\tilde{s}} \leq 5.04$  GeV. The latter corresponds, as is easy to see, to the laboratory photon energy domain  $\leq 13.05$  GeV. For the free total cross section  $\sigma_{\gamma p \rightarrow J/\psi p}(\sqrt{\tilde{s}})$  in this domain we have adopted the following expression [1], based on the predictions of the two gluon and three gluon exchange model [40] near threshold:

$$\sigma_{\gamma p \rightarrow J/\psi p}(\sqrt{\tilde{s}}) = \sigma_{2g}(\sqrt{\tilde{s}}) + \sigma_{3g}(\sqrt{\tilde{s}}), \quad (13)$$

where

$$\sigma_{2g}(\sqrt{\tilde{s}}) = a_{2g}(1-x)^2 \left[ \frac{e^{bt^+} - e^{bt^-}}{b} \right], \quad (14)$$

$$\sigma_{3g}(\sqrt{\tilde{s}}) = a_{3g}(1-x)^0 \left[ \frac{e^{bt^+} - e^{bt^-}}{b} \right] \quad (15)$$

and

$$x = (\tilde{s}_{\text{th}} - m_N^2)/(\tilde{s} - m_N^2). \quad (16)$$

Here,  $t^+$  and  $t^-$  are, respectively, the maximal and minimal values of the squared four-momentum

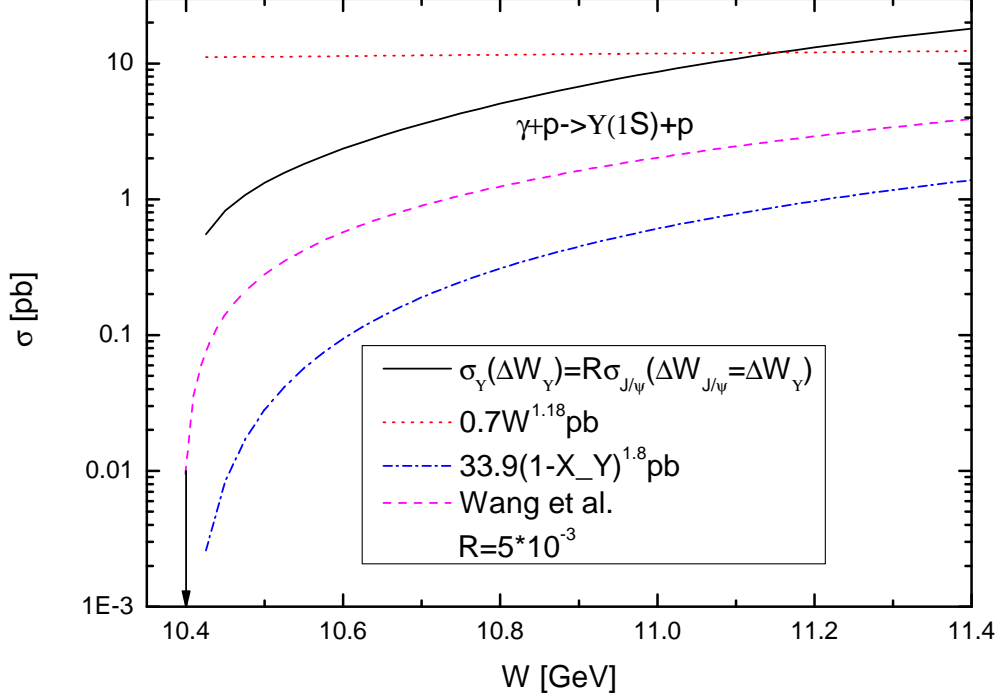


Figure 1: (Color online) The non-resonant total cross section for the reaction  $\gamma p \rightarrow \Upsilon(1S)p$  as a function of the center-of-mass energy  $W = \sqrt{s}$  of the photon–proton collisions. Solid, dashed, dotted-dashed and dotted curves are calculations by (10)–(20), within the dipole Pomeron model [21], by (22) and (24), respectively. The arrow indicates the center-of-mass threshold energy for direct  $\Upsilon(1S)$  photoproduction on a free target proton being at rest.

transfer  $t$  between the incident photon and the outgoing  $J/\psi$  meson. These values correspond to the  $t$  where the  $J/\psi$  is produced at angles of  $0^\circ$  and  $180^\circ$  in  $\gamma p$  c.m.s., respectively. They can readily be expressed in terms of the total energies and momenta of the initial photon and the  $J/\psi$  meson,  $E_\gamma^*, p_\gamma^*$  and  $E_{J/\psi}^*, p_{J/\psi}^*$ , in this system as follows:

$$t^\pm = m_{J/\psi}^2 - 2E_\gamma^*(m_N^2)E_{J/\psi}^*(m_{J/\psi}) \pm 2p_\gamma^*(m_N^2)p_{J/\psi}^*(m_{J/\psi}), \quad (17)$$

where

$$p_\gamma^*(m_N^2) = \frac{1}{2\sqrt{\tilde{s}}}\lambda(\tilde{s}, 0, m_N^2), \quad (18)$$

$$p_{J/\psi}^*(m_{J/\psi}) = \frac{1}{2\sqrt{\tilde{s}}}\lambda(\tilde{s}, m_{J/\psi}^2, m_N^2) \quad (19)$$

and

$$E_\gamma^*(m_N^2) = p_\gamma^*(m_N^2), \quad E_{J/\psi}^*(m_{J/\psi}) = \sqrt{m_{J/\psi}^2 + [p_{J/\psi}^*(m_{J/\psi})]^2}; \quad (20)$$

$$\lambda(x, y, z) = \sqrt{[x - (\sqrt{y} + \sqrt{z})^2][x - (\sqrt{y} - \sqrt{z})^2]}. \quad (21)$$

Parameter  $b$  in Eqs. (14), (15) is an exponential  $t$ -slope of the differential cross section of the reaction  $\gamma p \rightarrow J/\psi p$  near threshold [40]. According to [5],  $b \approx 1.67 \text{ GeV}^{-2}$ . We will employ this value in our calculations. The normalization coefficients  $a_{2g}$  and  $a_{3g}$  was determined in [1] as  $a_{2g} = 44.780 \text{ nb/GeV}^2$  and  $a_{3g} = 2.816 \text{ nb/GeV}^2$  assuming that incoherent sum (13) saturates the total experimental cross section of the reaction  $\gamma p \rightarrow J/\psi p$  measured at GlueX [5] at photon energies around 8.38 and 11.62 GeV.

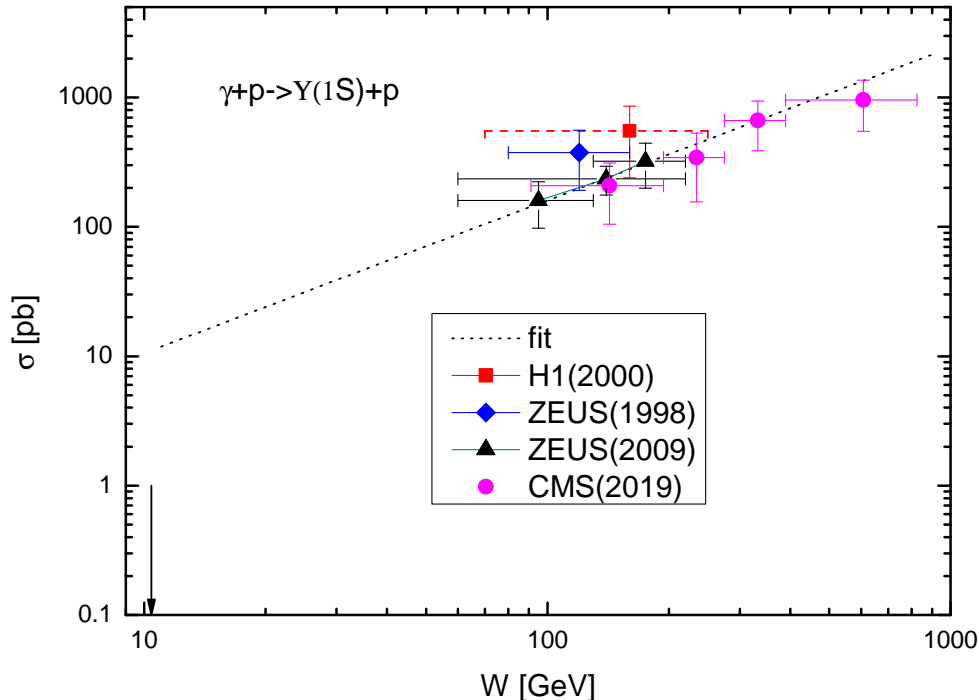


Figure 2: (Color online) The non-resonant total cross section for the reaction  $\gamma p \rightarrow \Upsilon(1S)p$  as a function of the center-of-mass energy  $W = \sqrt{s}$  of the photon–proton collisions. Dotted curve is calculation by (24). The experimental data are from Refs. [34–37]. The arrow indicates the center-of-mass threshold energy for direct  $\Upsilon(1S)$  photoproduction on a free target proton being at rest.

The results of calculations by Eqs. (10)–(20) of the non-resonant total cross section of the reaction  $\gamma p \rightarrow \Upsilon(1S)p$  at "low" energies are shown in Fig. 1 (solid curve). In this figure we also show the predictions from the dipole Pomeron model [21] (dashed curve)<sup>6)</sup> and from recently proposed parametrization [39]

$$\sigma_{\gamma p \rightarrow \Upsilon(1S)p}(\sqrt{s}) = 33.9(1 - x_{\Upsilon})^{1.8} \text{ [pb]}, \quad (22)$$

where  $x_{\Upsilon}$  is defined as

$$x_{\Upsilon} = (s_{\text{th}} - m_N^2)/(s - m_N^2) \quad (23)$$

(dotted-dashed curve). The results from the extrapolation of the fit [41]

$$\sigma_{\gamma p \rightarrow \Upsilon(1S)p}(\sqrt{s}) = 0.7(\sqrt{s})^{1.18} \text{ [pb]} \quad (24)$$

<sup>6)</sup>The author thanks X.-Y. Wang for sending these predictions to him.

of the high-energy data [36] (see Fig. 2<sup>7)</sup>) to threshold energies of interest are shown in Fig. 1 as well (dotted curve). It is, in particular, seen that at photon energies around 11 GeV our parametrization (10)–(20) is close to the results from the high-energy fit (24), and is considerably larger (by factors of about 5 and 15, respectively) than the results from the dipole Pomeron model [21] and from the parametrization (22). Therefore, the use of two parametrizations (10)–(20) and (22) in our subsequent calculations will give us the reasonable bounds for the elastic background under the pentaquark peaks. When they are employed in the calculations of the non-resonant  $\Upsilon(1S)$  photoproduction off nuclei presented below then, in line with above-mentioned, instead of the vacuum quantity  $s$ , appearing in Eqs. (10)–(12) and (23), one needs to adopt its in-medium expression (6) in which the laboratory incident photon energy  $E_\gamma$  is expressed via the given free space center-of-mass energy  $W$  as  $E_\gamma = (W^2 - m_N^2)/(2m_N)$ . And instead of the quantity  $m_N^2$ , entering into Eq. (18), we should employ the difference  $E_t^2 - p_t^2$ .

## 2.2. Two-step processes of resonant $\Upsilon(1S)$ photoproduction on nuclei

At photon center-of-mass energies  $\leq 11.4$  GeV, an incident photons can produce a non-strange charged  $P_b^+(11080)$ ,  $P_b^+(11125)$ ,  $P_b^+(11130)$  and neutral  $P_b^0(11080)$ ,  $P_b^0(11125)$ ,  $P_b^0(11130)$  resonances with pole masses  $M_{b1} = 11080$  MeV,  $M_{b2} = 11125$  MeV,  $M_{b3} = 11130$  MeV, respectively, predicted in Ref. [20] on the basis of the observed [2] three  $P_c^+$  states, in the first inelastic collisions with an intranuclear protons and neutrons<sup>8)</sup>:

$$\begin{aligned}\gamma + p &\rightarrow P_b^+(11080), \\ \gamma + p &\rightarrow P_b^+(11125), \\ \gamma + p &\rightarrow P_b^+(11130); \end{aligned} \tag{25}$$

$$\begin{aligned}\gamma + n &\rightarrow P_b^0(11080), \\ \gamma + n &\rightarrow P_b^0(11125), \\ \gamma + n &\rightarrow P_b^0(11130). \end{aligned} \tag{26}$$

Further, the produced intermediate pentaquarks can decay into the final states  $\Upsilon(1S)p$  and  $\Upsilon(1S)n$ :

$$\begin{aligned}P_b^+(11080) &\rightarrow \Upsilon(1S) + p, \\ P_b^+(11125) &\rightarrow \Upsilon(1S) + p, \\ P_b^+(11130) &\rightarrow \Upsilon(1S) + p; \end{aligned} \tag{27}$$

$$\begin{aligned}P_b^0(11080) &\rightarrow \Upsilon(1S) + n, \\ P_b^0(11125) &\rightarrow \Upsilon(1S) + n, \\ P_b^0(11130) &\rightarrow \Upsilon(1S) + n. \end{aligned} \tag{28}$$

Since the  $P_{bi}^+$  and  $P_{bi}^0$  states are not observed experimentally up to now, presently, neither their total decay widths  $\Gamma_{bi}$ , the branching ratios  $Br[P_{bi}^+ \rightarrow \Upsilon(1S)p]$  and  $Br[P_{bi}^0 \rightarrow \Upsilon(1S)n]$ <sup>9)</sup> of decays

<sup>7)</sup>Where also the data from other high-energy experiments [34, 35, 37] are given.

<sup>8)</sup>We recall that the threshold (resonant) energies  $E_\gamma^{R1}$ ,  $E_\gamma^{R2}$ ,  $E_\gamma^{R3}$  for the photoproduction of  $P_b^+(11080)$ ,  $P_b^+(11125)$ ,  $P_b^+(11130)$  and  $P_b^0(11080)$ ,  $P_b^0(11125)$ ,  $P_b^0(11130)$  resonances on a free target protons and neutrons being at rest are  $E_\gamma^{R1} = 64.952$  GeV,  $E_\gamma^{R2} = 65.484$  GeV,  $E_\gamma^{R3} = 65.544$  GeV and  $E_\gamma^{R1} = 64.863$  GeV,  $E_\gamma^{R2} = 65.395$  GeV,  $E_\gamma^{R3} = 65.454$  GeV, respectively.

<sup>9)</sup>Here,  $i=1, 2, 3$ .  $P_{b1}^+$ ,  $P_{b2}^+$ ,  $P_{b3}^+$  and  $P_{b1}^0$ ,  $P_{b2}^0$ ,  $P_{b3}^0$  stand for  $P_b^+(11080)$ ,  $P_b^+(11125)$ ,  $P_b^+(11130)$  and  $P_b^0(11080)$ ,  $P_b^0(11125)$ ,  $P_b^0(11130)$ , respectively.

(27) and (28) nor spin-parity quantum numbers are known in a model-independent way. Therefore, to estimate the  $\Upsilon(1S)$  production cross section from production/decay chains (25)–(28) one needs to rely on the theoretical predictions as well as on the similarity of the basic features of the decay properties of the  $qqqb\bar{b}$  and  $qqqc\bar{c}$  systems (with  $q = u$  or  $d$ ). Thus, the results for the decay rates of the modes (27), (28) are expressed in Ref. [20] in terms of the model parameter  $\Lambda$ , which should be constrained from the future experiments. The existence of the hidden-bottom pentaquark resonances with masses around 11 GeV and total decay widths from a few MeV to 45 MeV has been also predicted in Refs. [42–44]. With this and with above-mentioned, it is natural to assume, analogously to [41], for  $P_{bi}^+$  and  $P_{bi}^0$  states the same total widths  $\Gamma_{bi}$  as for their hidden-charm partners  $P_c^+(4312)$ ,  $P_c^+(4440)$  and  $P_c^+(4457)$ , i.e.,  $\Gamma_{b1} = 9.8$  MeV,  $\Gamma_{b2} = 20.6$  MeV,  $\Gamma_{b3} = 6.4$  MeV [2]. And for all branching ratios  $Br[P_{bi}^+ \rightarrow \Upsilon(1S)p]$  and  $Br[P_{bi}^0 \rightarrow \Upsilon(1S)n]$  of the decays (27) and (28) to adopt in our study the same [41] three main options:  $Br[P_{bi}^+ \rightarrow \Upsilon(1S)p] = 1, 2$  and  $3\%$  and  $Br[P_{bi}^0 \rightarrow \Upsilon(1S)n] = 1, 2$  and  $3\%$  as those used in Ref. [1] for the  $P_{ci}^+ \rightarrow J/\psi p$  decays. In order to see additionally the size of the impact of branching fractions  $Br[P_{bi}^+ \rightarrow \Upsilon(1S)p]$  and  $Br[P_{bi}^0 \rightarrow \Upsilon(1S)n]$  on the resonant  $\Upsilon(1S)$  yield in  $\gamma p \rightarrow \Upsilon(1S)p$ ,  $\gamma^{12}\text{C} \rightarrow \Upsilon(1S)X$  and  $\gamma^{208}\text{Pb} \rightarrow \Upsilon(1S)X$  reactions, we will also calculate this yield supposing that all these branching fractions are equal to 5 and 10% as well.

According to [1], majority of the  $P_{bi}^+$  and  $P_{bi}^0$  ( $i = 1, 2, 3$ ) resonances, having vacuum total decay widths in their rest frames  $\Gamma_{b1} = 9.8$  MeV,  $\Gamma_{b2} = 20.6$  MeV,  $\Gamma_{b3} = 6.4$  MeV, respectively, decay to  $\Upsilon(1S)p$  and  $\Upsilon(1S)n$  out of the target nuclei of interest. As in [1] for  $P_{ci}^+$  states, their free spectral functions are assumed to be described by the non-relativistic Breit-Wigner distributions:

$$S_{bi}^+(\sqrt{s}, \Gamma_{bi}) = S_{bi}^0(\sqrt{s}, \Gamma_{bi}) = \frac{1}{2\pi} \frac{\Gamma_{bi}}{(\sqrt{s} - M_{bi})^2 + \Gamma_{bi}^2/4}, \quad i = 1, 2, 3; \quad (29)$$

where  $\sqrt{s}$  is the total  $\gamma N$  c.m.s. energy defined above by Eq. (8). It should be pointed out that in case of calculating the excitation functions for production of  $P_{bi}^+$  and  $P_{bi}^0$  ( $i = 1, 2, 3$ ) resonances in reactions (25) and (26) on  $^{12}\text{C}$  and  $^{208}\text{Pb}$  targets in the "free"  $P_{bi}^+$  and  $P_{bi}^0$  spectral function scenario (see Fig. 4 below), this energy should be taken in form of Eq. (6). Spectral functions  $S_{bi}^+$  and  $S_{bi}^0$  correspond to the  $P_{bi}^+$  and  $P_{bi}^0$ , respectively. In line with [1], we assume that the in-medium spectral functions  $S_{bi}^+(\sqrt{s}, \Gamma_{\text{med}}^{bi})$ , and  $S_{bi}^0(\sqrt{s}, \Gamma_{\text{med}}^{bi})$  are also described by the Breit-Wigner formula (29) with a total in-medium widths  $\Gamma_{\text{med}}^{bi}$  ( $i = 1, 2, 3$ ) in their rest frames, obtained as a sum of the vacuum decay widths,  $\Gamma_{bi}$ , and averaged over local nucleon density  $\rho_N(\mathbf{r})$  collisional widths  $\langle \Gamma_{\text{coll},bi} \rangle$  appearing due to  $P_{bi}^+ N$ ,  $P_{bi}^0 N$  inelastic collisions:

$$\Gamma_{\text{med}}^{bi} = \Gamma_{bi} + \langle \Gamma_{\text{coll},bi} \rangle, \quad i = 1, 2, 3. \quad (30)$$

According to [4], the average collisional width  $\langle \Gamma_{\text{coll},bi} \rangle$  has a form:

$$\langle \Gamma_{\text{coll},bi} \rangle = \gamma_c v_c \sigma_{P_{bi}N} \langle \rho_N \rangle. \quad (31)$$

Here,  $\sigma_{P_{bi}N}$  is the  $P_{bi}^+$ ,  $P_{bi}^0$ -nucleon inelastic cross section <sup>10)</sup> and the Lorentz  $\gamma$ -factor  $\gamma_c$  and the velocity  $v_c$  of the resonances  $P_{bi}^+$ ,  $P_{bi}^0$  in the nuclear rest frame are determined by:

$$\gamma_c = \frac{(E_\gamma + E_t)}{\sqrt{s}}, \quad v_c = \frac{|\mathbf{p}_\gamma + \mathbf{p}_t|}{(E_\gamma + E_t)}. \quad (32)$$

<sup>10)</sup>Taking into account the quark contents of the hidden-charm and hidden-bottom pentaquarks as well as the fact that the nuclear medium suppresses  $\Upsilon(1S)$  production as much as  $J/\psi$  production, we will employ in the following calculations for the absorption cross section  $\sigma_{P_{bi}N}$  for each  $P_{bi}^+$  and  $P_{bi}^0$  ( $i = 1, 2, 3$ ) the same value of 33.5 mb as was adopted in Ref. [1] for the  $P_{ci}^+$ -nucleon absorption cross section.



Within the hadronic molecular scenario of  $P_{bi}^+$  and  $P_{bi}^0$  states <sup>11)</sup>, in which their spins-parities are  $J^P = (1/2)^-$  for  $P_{b1}^+$  and  $P_{b1}^0$ ,  $J^P = (1/2)^-$  for  $P_{b2}^+$  and  $P_{b2}^0$ ,  $J^P = (3/2)^-$  for  $P_{b3}^+$  and  $P_{b3}^0$  [20, 21], the free Breit-Wigner total cross sections for their production in reactions (25), (26) can be described on the basis of the spectral functions (29) and known branching fractions  $Br[P_{bi}^+ \rightarrow \gamma p]$  and  $Br[P_{bi}^0 \rightarrow \gamma n]$  ( $i=1, 2, 3$ ) as follows [41, 48]:

$$\begin{aligned}\sigma_{\gamma p \rightarrow P_{bi}^+}(\sqrt{s}, \Gamma_{bi}) &= f_{bi} \left( \frac{\pi}{p_\gamma^*} \right)^2 Br[P_{bi}^+ \rightarrow \gamma p] S_{bi}^+(\sqrt{s}, \Gamma_{bi}) \Gamma_{bi}, \\ \sigma_{\gamma n \rightarrow P_{bi}^0}(\sqrt{s}, \Gamma_{bi}) &= f_{bi} \left( \frac{\pi}{p_\gamma^*} \right)^2 Br[P_{bi}^0 \rightarrow \gamma n] S_{bi}^0(\sqrt{s}, \Gamma_{bi}) \Gamma_{bi}.\end{aligned}\quad (33)$$

Here, the center-of-mass 3-momentum in the incoming  $\gamma N$  channel,  $p_\gamma^*$ , is defined above by Eq. (18) in which one has to make the substitution  $\tilde{s} \rightarrow s$  and the ratios of spin factors  $f_{b1} = 1$ ,  $f_{b2} = 1$ ,  $f_{b3} = 2$ .

In line with [1, 41, 49], we assume that the  $P_{b1}^+$  and  $P_{b1}^0$  ( $1/2$ )<sup>-</sup>,  $P_{b2}^+$  and  $P_{b2}^0$  ( $1/2$ )<sup>-</sup>, and  $P_{b3}^+$  and  $P_{b3}^0$  ( $3/2$ )<sup>-</sup> decays to  $\Upsilon(1S)p$  and  $\Upsilon(1S)n$  are dominated by the lowest partial waves with relative orbital angular momentum  $L = 0$ . Then, the branching fractions  $Br[P_{bi}^+ \rightarrow \gamma p]$  and  $Br[P_{bi}^0 \rightarrow \gamma n]$  can be expressed, adopting the vector-meson dominance model, respectively, through the branching ratios  $Br[P_{bi}^+ \rightarrow \Upsilon(1S)p]$  and  $Br[P_{bi}^0 \rightarrow \Upsilon(1S)n]$  in the following manner [1, 41, 48, 49]:

$$\begin{aligned}Br[P_{bi}^+ \rightarrow \gamma p] &= 4\pi\alpha \left( \frac{f_\Upsilon}{m_{\Upsilon(1S)}} \right)^2 f_{0,bi} \left( \frac{p_{\Upsilon,bi}^*}{p_{\Upsilon,bi}^*} \right) Br[P_{bi}^+ \rightarrow \Upsilon(1S)p], \\ Br[P_{bi}^0 \rightarrow \gamma n] &= 4\pi\alpha \left( \frac{f_\Upsilon}{m_{\Upsilon(1S)}} \right)^2 f_{0,bi} \left( \frac{p_{\Upsilon,bi}^*}{p_{\Upsilon,bi}^*} \right) Br[P_{bi}^0 \rightarrow \Upsilon(1S)n],\end{aligned}\quad (34)$$

where  $f_\Upsilon = 238$  MeV [41] is the  $\Upsilon(1S)$  decay constant,  $\alpha = 1/137$  is the electromagnetic fine structure constant and

$$p_{\gamma,bi}^* = \frac{1}{2M_{bi}} \lambda(M_{bi}^2, 0, m_N^2), \quad p_{\Upsilon,bi}^* = \frac{1}{2M_{bi}} \lambda(M_{bi}^2, m_{\Upsilon(1S)}^2, m_N^2), \quad (35)$$

$$f_{0,bi} = \frac{2}{2 + \gamma_{bi}^2}, \quad \gamma_{bi}^2 = 1 + p_{\Upsilon,bi}^{*2}/m_{\Upsilon(1S)}^2. \quad (36)$$

Accounting for that  $Br[P_{bi}^+ \rightarrow \Upsilon(1S)p] = Br[P_{bi}^0 \rightarrow \Upsilon(1S)n]$  [20], we obtain from Eqs. (34)–(36) that

$$Br[P_{bi}^0 \rightarrow \gamma n] = Br[P_{bi}^+ \rightarrow \gamma p]. \quad (37)$$

With Eq. (33) and with this, we have:

$$\sigma_{\gamma p \rightarrow P_{bi}^+}(\sqrt{s}, \Gamma_{bi}) = \sigma_{\gamma n \rightarrow P_{bi}^0}(\sqrt{s}, \Gamma_{bi}). \quad (38)$$

Eqs. (35), (36) yield that  $(p_{\gamma,b1}^*, p_{\Upsilon,b1}^*, f_{0,b1}) = (5.500$  GeV/c, 1.223 GeV/c, 0.663),  $(p_{\gamma,b2}^*, p_{\Upsilon,b2}^*, f_{0,b2}) = (5.523$  GeV/c, 1.271 GeV/c, 0.663) and  $(p_{\gamma,b3}^*, p_{\Upsilon,b3}^*, f_{0,b3}) = (5.526$  GeV/c, 1.277 GeV/c, 0.663). As a result, we get from Eq. (34):

$$\begin{aligned}Br[P_{b1}^+ \rightarrow \gamma p] &= 1.73 \cdot 10^{-4} Br[P_{b1}^+ \rightarrow \Upsilon(1S)p], \\ Br[P_{b2}^+ \rightarrow \gamma p] &= 1.67 \cdot 10^{-4} Br[P_{b2}^+ \rightarrow \Upsilon(1S)p], \\ Br[P_{b3}^+ \rightarrow \gamma p] &= 1.67 \cdot 10^{-4} Br[P_{b3}^+ \rightarrow \Upsilon(1S)p].\end{aligned}\quad (39)$$

<sup>11)</sup>In this scenario, due to the proximity of the predicted  $P_{b1}^+$ ,  $P_{b1}^0$  and  $P_{b2}^+$ ,  $P_{b2}^0$ ,  $P_{b3}^+$ ,  $P_{b3}^0$  masses to the  $\Sigma_b B$  and  $\Sigma_b B^*$  thresholds [20], the  $P_{b1}^+$ ,  $P_{b1}^0$  resonances can be considered as the  $\Sigma_b B$  bound states, while the  $P_{b2}^+$ ,  $P_{b2}^0$  and  $P_{b3}^+$ ,  $P_{b3}^0$  as  $\Sigma_b B^*$  bound molecular systems [20, 41–47].

The free total cross sections  $\sigma_{\gamma p \rightarrow P_{bi}^+ \rightarrow \Upsilon(1S)p}(\sqrt{s}, \Gamma_{bi})$  and  $\sigma_{\gamma n \rightarrow P_{bi}^0 \rightarrow \Upsilon(1S)n}(\sqrt{s}, \Gamma_{bi})$  for resonant  $\Upsilon(1S)$  production in the two-step processes (25)–(28) can be represented in the following forms [1, 4]:

$$\sigma_{\gamma p \rightarrow P_{bi}^+ \rightarrow \Upsilon(1S)p}(\sqrt{s}, \Gamma_{bi}) = \sigma_{\gamma p \rightarrow P_{bi}^+}(\sqrt{s}, \Gamma_{bi})\theta[\sqrt{s} - (m_{\Upsilon(1S)} + m_N)]Br[P_{bi}^+ \rightarrow \Upsilon(1S)p], \quad (40)$$

$$\sigma_{\gamma n \rightarrow P_{bi}^0 \rightarrow \Upsilon(1S)n}(\sqrt{s}, \Gamma_{bi}) = \sigma_{\gamma n \rightarrow P_{bi}^0}(\sqrt{s}, \Gamma_{bi})\theta[\sqrt{s} - (m_{\Upsilon(1S)} + m_N)]Br[P_{bi}^0 \rightarrow \Upsilon(1S)n]. \quad (41)$$

Here,  $\theta(x)$  is the usual step function. According to Eqs. (33), (34) and (38) these cross sections are equal to each other and they are proportional to  $Br^2[P_{bi}^+ \rightarrow \Upsilon(1S)p]$  and  $Br^2[P_{bi}^0 \rightarrow \Upsilon(1S)n]$ , respectively.

According to [1, 4], we obtain the following expression for the total cross section for  $\Upsilon(1S)$  production in  $\gamma A$  interactions from the chains (25)–(28):

$$\sigma_{\gamma A \rightarrow \Upsilon(1S)X}^{(\text{sec})}(E_\gamma) = \sum_{i=1}^3 \left[ \sigma_{\gamma A \rightarrow P_{bi}^+ \rightarrow \Upsilon(1S)p}^{(\text{sec})}(E_\gamma) + \sigma_{\gamma A \rightarrow P_{bi}^0 \rightarrow \Upsilon(1S)n}^{(\text{sec})}(E_\gamma) \right], \quad (42)$$

where

$$\begin{aligned} \sigma_{\gamma A \rightarrow P_{bi}^+ \rightarrow \Upsilon(1S)p}^{(\text{sec})}(E_\gamma) &= \left( \frac{Z}{A} \right) I_V[A, \sigma_{P_{bi}N}^{\text{eff}}] \langle \sigma_{\gamma p \rightarrow P_{bi}^+}(E_\gamma) \rangle_A Br[P_{bi}^+ \rightarrow \Upsilon(1S)p], \\ \sigma_{\gamma A \rightarrow P_{bi}^0 \rightarrow \Upsilon(1S)n}^{(\text{sec})}(E_\gamma) &= \left( \frac{N}{A} \right) I_V[A, \sigma_{P_{bi}N}^{\text{eff}}] \langle \sigma_{\gamma n \rightarrow P_{bi}^0}(E_\gamma) \rangle_A Br[P_{bi}^0 \rightarrow \Upsilon(1S)n] \end{aligned} \quad (43)$$

and

$$\begin{aligned} \langle \sigma_{\gamma n \rightarrow P_{bi}^0}(E_\gamma) \rangle_A &= \langle \sigma_{\gamma p \rightarrow P_{bi}^+}(E_\gamma) \rangle_A \\ &= \int \int P_A(\mathbf{p}_t, E) d\mathbf{p}_t dE \sigma_{\gamma p \rightarrow P_{bi}^+}(\sqrt{s_{\Upsilon(1S)}}, \Gamma_{\text{med}}^{bi})\theta[\sqrt{s_{\Upsilon(1S)}} - (m_{\Upsilon(1S)} + m_N)]. \end{aligned} \quad (44)$$

Here,  $\sigma_{\gamma p \rightarrow P_{bi}^+}(\sqrt{s_{\Upsilon(1S)}}, \Gamma_{\text{med}}^{bi})$  is the "in-medium" cross section for the  $P_{bi}^+$  resonance production in  $\gamma p$  collisions (25),  $Z$  and  $N$  are the numbers of protons and neutrons in the target nucleus. As above in Eq. (29), we assume that this cross section is equivalent to the free cross section of Eq. (33) in which the vacuum decay width  $\Gamma_{bi}$  is replaced by the in-medium width  $\Gamma_{\text{med}}^{bi}$  as given by Eqs. (30)–(32) and vacuum center-of-mass energy squared  $s$ , presented by the formula (8), is replaced by the in-medium expression (6). The quantity  $I_V[A, \sigma_{P_{bi}N}^{\text{eff}}]$  in Eq. (43) is defined above by Eq. (4) in which one needs to make the substitution  $\sigma \rightarrow \sigma_{P_{bi}N}^{\text{eff}}$ . Here,  $\sigma_{P_{bi}N}^{\text{eff}}$  is the  $P_{bi}^+$ ,  $P_{bi}^0$ -nucleon effective absorption cross section. This cross section can be represented [1, 4] as a sum of the inelastic cross section  $\sigma_{P_{bi}N}$ , introduced above, and the additional to this cross section effective  $P_{bi}^+$ ,  $P_{bi}^0$  absorption cross section associated with their decays in the nucleus. From the standpoint of generality, we assume that the cross section  $\sigma_{P_{bi}N}^{\text{eff}}$  has the same value of 37 mb as was adopted in Ref. [1] for the  $P_{ci}^+$ -nucleon effective absorption cross section  $\sigma_{P_{ci}N}^{\text{eff}}$ .

### 3. Numerical results and discussion

The free elementary non-resonant  $\Upsilon(1S)$  production cross section in the reaction  $\gamma p \rightarrow \Upsilon(1S)p$ , determined on the basis of Eqs. (22) (left panel) and (10)–(20) (right panel), and the combined (non-resonant plus resonant (40)) total cross sections are presented in Fig. 3. From this figure, one can see that the  $P_b^+(11080)$  state appears as clear narrow independent peak at  $E_\gamma = 64.95$  GeV in the combined cross section, while the  $P_b^+(11125)$  and  $P_b^+(11130)$  resonances exhibit itself here, due to low distance between their centroids (60 MeV), as one distinct wide peak at  $E_\gamma \approx 65.50$  GeV for two adopted choices (10)–(20) and (22) for the background contribution, if  $Br[P_{bi}^+ \rightarrow \Upsilon(1S)p] = 2, 3, 5$  and 10% ( $i = 1, 2, 3$ ). In these cases, at laboratory photon energies around the peak energies

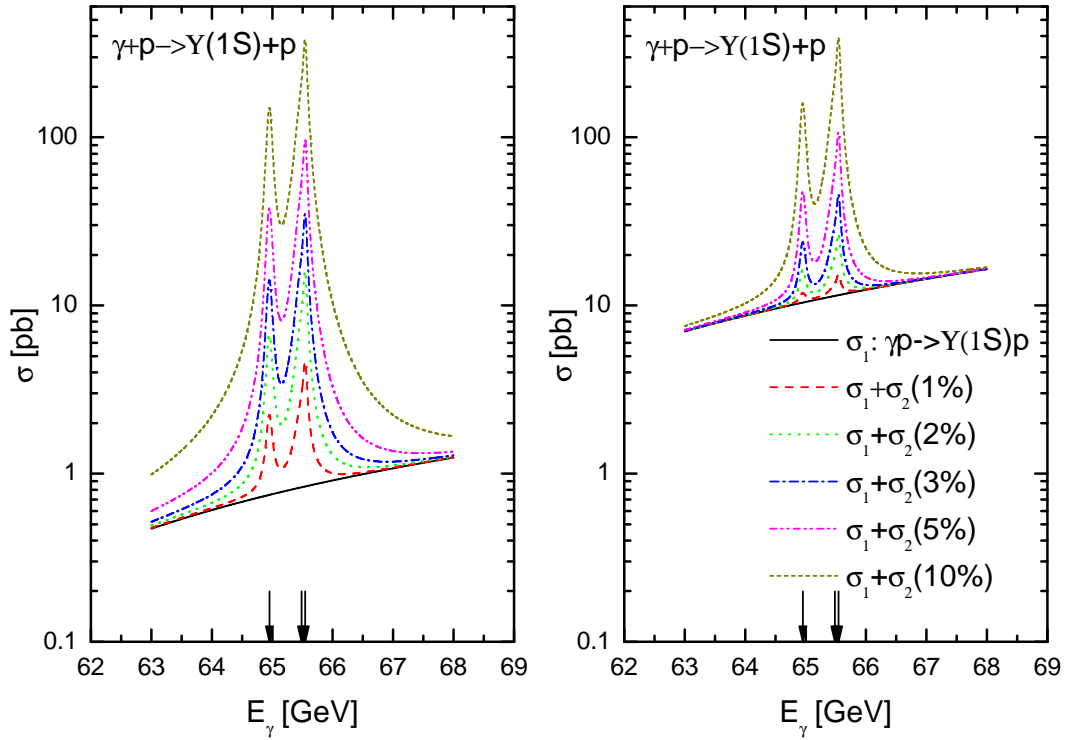


Figure 3: (Color online) The non-resonant total cross section for the reaction  $\gamma p \rightarrow \Upsilon(1S)p$  (solid curves), calculated on the basis of Eqs. (22) (left panel) and (10)–(20) (right panel). Incoherent sum of it and the total cross section for the resonant  $\Upsilon(1S)$  production in the processes  $\gamma p \rightarrow P_{bi}^+ \rightarrow \Upsilon(1S)p$ , ( $i = 1, 2, 3$ ), calculated assuming that the resonances  $P_{b1}^+$ ,  $P_{b2}^+$  and  $P_{b3}^+$  with the spin-parity quantum numbers  $J^P = (1/2)^-$ ,  $J^P = (1/2)^-$  and  $J^P = (3/2)^-$  decay to  $\Upsilon(1S)p$  with the lower allowed relative orbital angular momentum  $L = 0$  with all three branching fractions  $Br[P_{bi}^+ \rightarrow \Upsilon(1S)p] = 1, 2, 3, 5$  and  $10\%$  (respectively, dashed, dotted, dashed-dotted, dashed-dotted-dotted and short-dashed curves), as functions of laboratory photon energy  $E_\gamma$ . The three arrows indicate the resonant energies  $E_\gamma^{\text{R1}} = 64.952$  GeV,  $E_\gamma^{\text{R2}} = 65.484$  GeV and  $E_\gamma^{\text{R3}} = 65.544$  GeV.

the resonant contributions are much larger than the non-resonant ones. Therefore, the background reaction will not influence the direct observation of the hidden-bottom pentaquark production at these energies. The peak values of the combined cross section reach tens and hundreds of picobarns, if  $Br[P_{bi}^+ \rightarrow \Upsilon(1S)p] = 2$  and  $10\%$ , respectively<sup>12)</sup>. But, they are much smaller than those of a few nanobarns for the reaction  $\gamma p \rightarrow J/\psi p$  with  $P_{ci}^+$  production [1]. This requires both the very high luminosities, which will be accessible at future facilities such as proposed electron–ion colliders EIC [22–24] and EicC [25, 26] in the U.S. and China, and large-acceptance detectors. The strengths of these two peaks, obtained for  $Br[P_{bi}^+ \rightarrow \Upsilon(1S)p] = 1\%$ , decrease essentially compared to the above cases and have a peak values of about 2, 5 pb and 12, 15 pb for background contribution in the form of (22) and (10)–(20), respectively. But, in former case, the  $P_b^+$  signal to background ratio is larger than that in the latter case by about of one order of magnitude. Therefore, it is natural to expect that this signal can be distinguished from the background reaction as well, if it has the

<sup>12)</sup>It should be pointed out that the peak strengths of the combined cross section of the reaction  $\gamma p \rightarrow \Upsilon(1S)p$ , corresponding to the  $P_b^+(11080)$  and  $P_b^+(11125)$  states and obtained within the dipole Pomeron model in Ref. [21], are about of 3 and 8 nb, respectively. These are much larger than those determined in the present work.

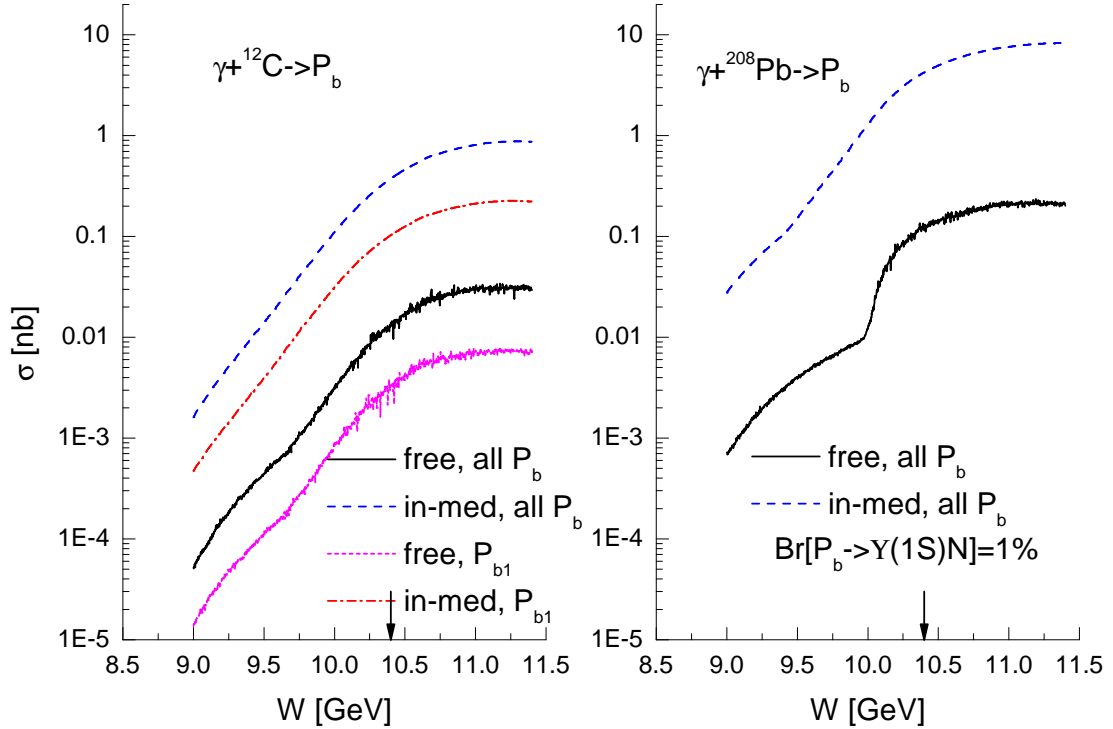


Figure 4: (Color online) Excitation functions for resonant production of  $P_{bi}^+$  and  $P_{bi}^0$  ( $i = 1, 2, 3$ ) states off  $^{12}\text{C}$  and  $^{208}\text{Pb}$  from the processes  $\gamma p \rightarrow P_{bi}^+$  and  $\gamma n \rightarrow P_{bi}^0$ , respectively, going on off-shell target nucleons, calculated for  $Br[P_{bi}^+ \rightarrow \Upsilon(1S)p] = Br[P_{bi}^0 \rightarrow \Upsilon(1S)n] = 1\%$  for all  $i$  adopting free (solid curves) and in-medium (dashed curves)  $P_{bi}^+$ ,  $P_{bi}^0$  spectral functions.  $^{12}\text{C}$  case: the same as above, but only for the processes  $\gamma p \rightarrow P_{b1}^+$  and  $\gamma n \rightarrow P_{b1}^0$ , employing free (short-dashed) and in-medium (dotted-dashed)  $P_{b1}^+$  and  $P_{b1}^0$  spectral functions. The arrows indicate the threshold center-of-mass energy for direct  $\Upsilon(1S)$  photoproduction on a free target nucleon being at rest.

cross section of about 1 pb in the energy region around energies  $E_\gamma = 64.95$  and  $E_\gamma = 65.50$  GeV. To see experimentally such two-peak structure in the combined total cross section of the reaction  $\gamma p \rightarrow \Upsilon(1S)p$ <sup>13)</sup>, it is enough to have the photon energy resolution and energy binning of the order of 20–30 MeV<sup>14)</sup>. Thus, the c.m. energy ranges  $M_{bi} - \Gamma_{bi}/2 < \sqrt{s} < M_{bi} + \Gamma_{bi}/2$  ( $i = 1, 2$ ) correspond to laboratory photon energy regions of  $64.894 \text{ GeV} < E_\gamma < 65.010 \text{ GeV}$  and  $65.362 \text{ GeV} < E_\gamma < 65.607 \text{ GeV}$ , i.e.  $\Delta E_\gamma = 116$  and  $245$  MeV for  $P_b^+(11080)$  and  $P_b^+(11125)$ , respectively. This means that to resolve the two peaks in Fig. 3 the photon energy resolution and the energy bin size of the order of 20–30 MeV are required. Finally, it is worth noting that the measurement of elastic bottomonium production on proton close to threshold at electron-ion colliders will allow to determine the contribution of the so-called trace anomaly term to the proton mass as well [50]. It has not been determined yet experimentally, nor by a lattice QCD calculations [50]. The determination of this contribution would enable us to better understand the origin of the total mass of the nucleon in terms of its constituents (quarks and gluons). And in addition, it should be mentioned that the use of bottomonium production at large  $W$  should allow one to shed light also on the contribution

<sup>13)</sup>The  $\Upsilon(1S)$  mesons could be identified via the muonic decays  $\Upsilon(1S) \rightarrow \mu^+\mu^-$  with a branching ratio of 2.48% [34].

<sup>14)</sup>It should be noticed that, for example, in the GlueX experiment [5] the  $E_\gamma$  resolution was 20 MeV for a 10 GeV photon.

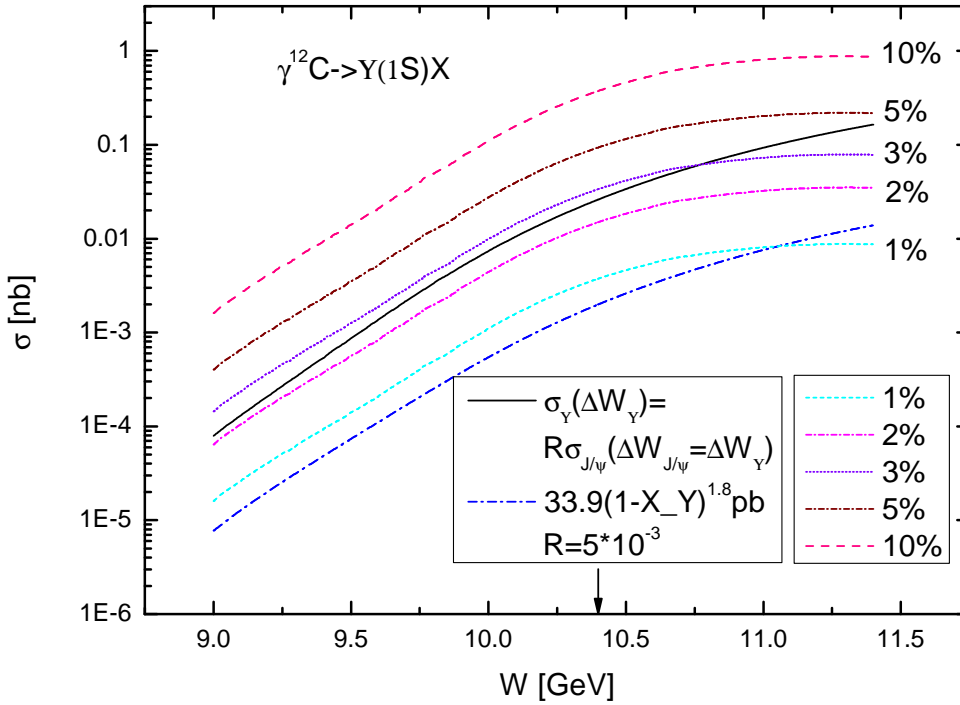


Figure 5: (Color online) Excitation functions for the non-resonant and resonant production of  $\Upsilon(1S)$  mesons off  $^{12}\text{C}$  from direct  $\gamma N \rightarrow \Upsilon(1S)N$  and resonant  $\gamma p \rightarrow P_{bi}^+ \rightarrow \Upsilon(1S)p$  and  $\gamma n \rightarrow P_{bi}^0 \rightarrow \Upsilon(1S)n$  ( $i = 1, 2, 3$ ) reactions going on off-shell target nucleons. The curves (solid and dotted-dashed), corresponding to the non-resonant production of  $\Upsilon(1S)$  mesons, are calculations by (3) with elementary cross section  $\sigma_{\gamma p \rightarrow \Upsilon(1S)p}$  in the forms of (10)–(20) and (22), respectively. The curves, belonging to their resonant production, are calculations by (42) for branching ratios  $Br[P_{bi}^+ \rightarrow \Upsilon(1S)p] = Br[P_{bi}^0 \rightarrow \Upsilon(1S)n] = 1, 2, 3, 5$  and 10% for all  $i$  adopting in-medium  $P_{bi}^+$ ,  $P_{bi}^0$  spectral functions. The arrow indicates the threshold center-of-mass energy for direct  $\Upsilon(1S)$  photoproduction on a free target nucleus being at rest.

of the total gluon angular momentum to the proton spin [50].

Figure 4 shows the energy dependences of the total  $P_{b1}^+$ ,  $P_{b2}^+$ ,  $P_{b3}^+$  and  $P_{b1}^0$ ,  $P_{b2}^0$ ,  $P_{b3}^0$  production cross section in  $\gamma^{12}\text{C}$  and  $\gamma^{208}\text{Pb}$  reactions as well as of the total  $P_{b1}^+$ ,  $P_{b1}^0$  creation in  $\gamma^{12}\text{C}$  collisions. They are calculated on the basis of Eqs. (42), (43)<sup>15)</sup> in the scenarios with free and in-medium  $P_{bi}^+$  and  $P_{bi}^0$  spectral functions for branching ratios  $Br[P_{bi}^+ \rightarrow \Upsilon(1S)p] = Br[P_{bi}^0 \rightarrow \Upsilon(1S)n] = 1\%$  ( $i = 1, 2, 3$ ). It is seen that the hidden-bottom pentaquark resonance formation is smeared out by Fermi motion of intranuclear nucleons. It is a substantially enhanced for the in-medium case at all photon c.m.s. energies considered. As is also easy to see, the contribution to the  $\Upsilon(1S)$  production on nuclei, which will come from the intermediate  $P_b^+(11080)$  and  $P_b^0(11080)$  states, amounts approximately 25% both at subthreshold incident energies ( $W < 10.4$  GeV) and at above threshold beam energies ( $W > 10.4$  GeV).

Excitation functions for non-resonant production of  $\Upsilon(1S)$  mesons as well as for their resonant production via  $P_{b1}^+$ ,  $P_{b2}^+$ ,  $P_{b3}^+$  and  $P_{b1}^0$ ,  $P_{b2}^0$ ,  $P_{b3}^0$  resonances formation and decay in  $\gamma^{12}\text{C}$  and  $\gamma^{208}\text{Pb}$  collisions are given in Figs. (5) and (6), respectively. The former ones are calculated using Eq. (3) for

<sup>15)</sup>By assuming that in Eq. (43)  $Br[P_{bi}^+ \rightarrow \Upsilon(1S)p] = Br[P_{bi}^0 \rightarrow \Upsilon(1S)n] = 1$  for all  $i$  considered.

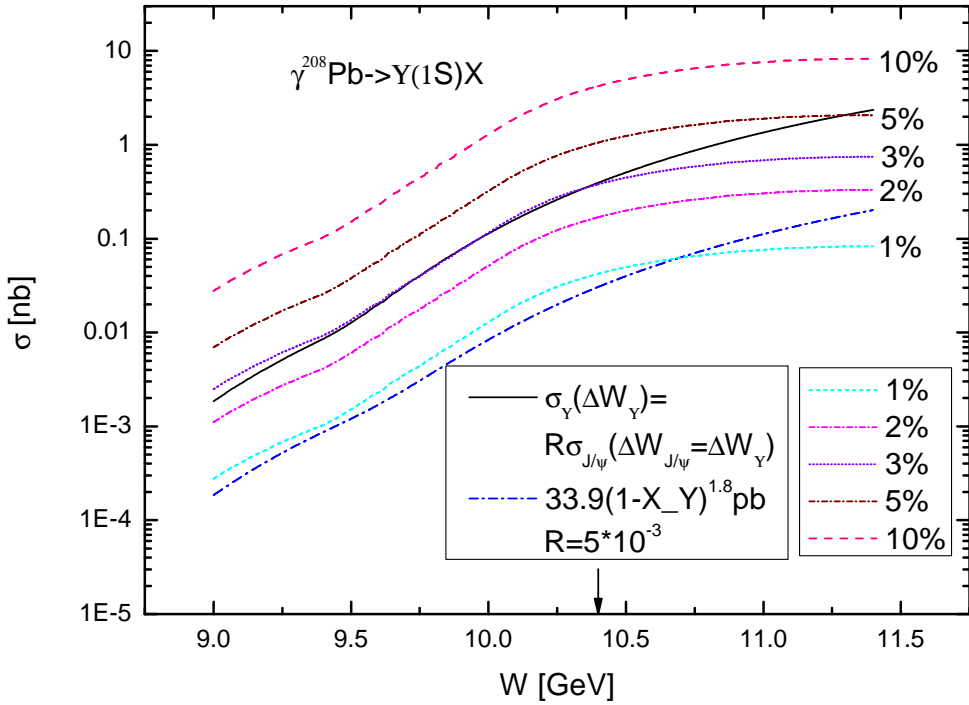


Figure 6: (Color online) The same as in figure 5, but for the  $^{208}\text{Pb}$  target nucleus.

two employed options (10)–(20) and (22) for the non-resonant elementary cross section  $\sigma_{\gamma p \rightarrow \Upsilon(1S)p}$ , whereas the latter ones are determined using Eqs. (42), (43) in the in-medium  $P_{bi}^+$  and  $P_{bi}^0$  spectral functions scenario and assuming that for all  $i$  branching ratios  $Br[P_{bi}^+ \rightarrow \Upsilon(1S)p] = Br[P_{bi}^0 \rightarrow \Upsilon(1S)n] = 1, 2, 3, 5$  and  $10\%$ . One can see that the non-resonant  $\Upsilon(1S)$  yield and that from the production and decay of the intermediate  $P_{bi}^+$  and  $P_{bi}^0$  resonances are comparable for both considered target nuclei if  $Br[P_{bi}^+ \rightarrow \Upsilon(1S)p] = Br[P_{bi}^0 \rightarrow \Upsilon(1S)n] = 1$  and  $3\%$  when the background cross section  $\sigma_{\gamma p \rightarrow \Upsilon(1S)p}$  is used in the forms of (22) and (10)–(20), respectively. But, if these branching ratios are more than 1 and  $3\%$ , correspondingly, the resonant  $\Upsilon(1S)$  production cross section is much larger, especially at subthreshold beam energies, than the non-resonant one and their relative strength is governed by the ratios.

Thus, the presence of the  $P_{bi}^+$  and  $P_{bi}^0$  pentaquark states leads to additional (and essential) enhancement in the behavior of the total  $\Upsilon(1S)$  production cross section on nuclei both below and above threshold and the strength of this enhancement is strongly determined by the branching fractions of their decays to  $\Upsilon(1S)p$  and  $\Upsilon(1S)n$  final states, respectively. These fractions can be accurately studied experimentally at electron-ion colliders also via the bottomonium excitation function measurements on nuclear targets near threshold and comparison their results with the calculations on the basis of the present model with known total cross sections of direct processes (1) and (2)<sup>16)</sup>. The collected statistics in these measurements, especially on heavy target nuclei and at above threshold energies where the resonant  $\Upsilon(1S)$  production cross section reaches the values  $\sim 1$ – $10$  nb for above branching fractions  $\sim 5$ – $10\%$ , is expected to be substantially higher than that, which could be achieved in measurements on the nucleon target (cf. Figs. 5, 6 and 3). This should

<sup>16)</sup>If these cross sections are different, then in Eq. (3) one needs to perform the following substitution  $\langle \sigma_{\gamma p \rightarrow \Upsilon(1S)p}(E_\gamma) \rangle_A \rightarrow (Z/A) \langle \sigma_{\gamma p \rightarrow \Upsilon(1S)p}(E_\gamma) \rangle_A + (N/A) \langle \sigma_{\gamma n \rightarrow \Upsilon(1S)n}(E_\gamma) \rangle_A$ .

enable a more accurate determination of these fractions in the measurements on nuclear targets.

## 4. Summary

In this work we have calculated the absolute excitation functions for the non-resonant and resonant photoproduction of  $\Upsilon(1S)$  mesons off protons at threshold incident photon laboratory energies of 63–68 GeV by accounting for direct ( $\gamma p \rightarrow \Upsilon(1S)p$ ) and two-step ( $\gamma p \rightarrow P_b^+(11080) \rightarrow \Upsilon(1S)p$ ,  $\gamma p \rightarrow P_b^+(11125) \rightarrow \Upsilon(1S)p$ ,  $\gamma p \rightarrow P_b^+(11130) \rightarrow \Upsilon(1S)p$ )  $\Upsilon(1S)$  production channels within different scenarios for the non-resonant total cross section of elementary reaction  $\gamma p \rightarrow \Upsilon(1S)p$  and for branching ratios of the decays  $P_b^+(11080) \rightarrow \Upsilon(1S)p$ ,  $P_b^+(11125) \rightarrow \Upsilon(1S)p$ ,  $P_b^+(11130) \rightarrow \Upsilon(1S)p$ . Also, an analogous functions for photoproduction of  $\Upsilon(1S)$  mesons on  $^{12}\text{C}$  and  $^{208}\text{Pb}$  target nuclei in the near-threshold center-of-mass beam energy region of 9.0–11.4 GeV have been calculated by considering incoherent direct ( $\gamma N \rightarrow \Upsilon(1S)N$ ) and two-step ( $\gamma p \rightarrow P_b^+(11080) \rightarrow \Upsilon(1S)p$ ,  $\gamma p \rightarrow P_b^+(11125) \rightarrow \Upsilon(1S)p$ ,  $\gamma p \rightarrow P_b^+(11130) \rightarrow \Upsilon(1S)p$  and  $\gamma n \rightarrow P_b^0(11080) \rightarrow \Upsilon(1S)n$ ,  $\gamma n \rightarrow P_b^0(11125) \rightarrow \Upsilon(1S)n$ ,  $\gamma n \rightarrow P_b^0(11130) \rightarrow \Upsilon(1S)n$ )  $\Upsilon(1S)$  production processes within a nuclear spectral function approach. It was shown that the  $P_b^+(11080)$  state appears as clear narrow independent peak at  $E_\gamma = 64.95$  GeV in the combined (non-resonant plus resonant) cross section on proton target, while the  $P_b^+(11125)$  and  $P_b^+(11130)$  resonances exhibit itself here, due to low distance between their centroids (60 MeV), as one distinct wide peak at  $E_\gamma \approx 65.50$  GeV for two adopted options for the background contribution, if  $Br[P_{bi}^+ \rightarrow \Upsilon(1S)p] = 2, 3, 5$  and 10% ( $i = 1, 2, 3$ ). The peak values of the combined cross section reach tens and hundreds of picobarns, if  $Br[P_{bi}^+ \rightarrow \Upsilon(1S)p] = 2$  and 10%, respectively. Therefore, a detailed scan of the  $\Upsilon(1S)$  total photoproduction cross section on a proton target in the near-threshold energy region in future high-precision experiments at electron-ion colliders should give a definite result for or against the existence of the non-strange hidden-bottom pentaquark states and clarify their decay rates.

It was also demonstrated that the presence of the  $P_{bi}^+$  and  $P_{bi}^0$  pentaquark states in  $\Upsilon(1S)$  photoproduction on nuclei leads to additional (and essential) enhancement in the behavior of the total  $\Upsilon(1S)$  production cross section on nuclei both below and above threshold and the strength of this enhancement is strongly determined by the branching fractions of their decays to  $\Upsilon(1S)p$  and  $\Upsilon(1S)n$  final states, respectively. This offers an indirect possibility of studying of these fractions experimentally at the future high-luminosity electron-ion colliders EIC and EicC in the U.S. and China also via the near-threshold bottomonium excitation function measurements on nuclear targets. The collected statistics in these measurements, especially on heavy target nuclei and at above threshold energies where the resonant  $\Upsilon(1S)$  production cross section reaches the values  $\sim 1$ –10 nb for above branching fractions  $\sim 5$ –10%, is expected to be substantially higher than that, which could be achieved in measurements on the nucleon target. This should enable a more accurate determination of these fractions in the measurements on nuclear targets.

## References

- [1] E. Ya. Paryev, Nucl. Phys. A **996**, 121711 (2020); arXiv:2003.00788 [nucl-th].
- [2] R. Aaij *et al.* (LHCb Collaboration), Phys. Rev. Lett. **122**, 222001 (2019); arXiv:1904.03947 [hep-ex].
- [3] R. Aaij *et al.* (LHCb Collaboration), Phys. Rev. Lett. **115**, 072001 (2015); arXiv:1507.03414 [hep-ex].

- [4] E. Ya. Paryev and Yu.T. Kiselev, Nucl. Phys. A **978**, 201 (2018); arXiv:1810.01715 [nucl-th].
- [5] A. Ali *et al.* (The GlueX Collaboration), Phys. Rev. Lett. **123**, 072001 (2019); arXiv:1905.10811 [nucl-ex].
- [6] X.-Y. Wang, X.-R. Chen, and J. He, Phys. Rev. D **99**, 114007 (2019).
- [7] X.-Y. Wang *et al.*, Phys. Lett. B **797**, 134862 (2019); arXiv:1906.04044 [hep-ph].
- [8] C.-J. Xiao *et al.*, Phys. Rev. D **100**, 014022 (2019).
- [9] A. Ali *et al.*, arXiv:1907.06507 [hep-ph].
- [10] H. X. Chen, W. Chen and S.-L. Zhu, Phys. Rev. D **100**, 051501 (2019); arXiv:1903.11001 [hep-ph].
- [11] R. Chen, Z. F. Sun, X. Liu and S.-L. Zhu, Phys. Rev. D **100**, 011502 (2019); arXiv:1903.11013 [hep-ph].
- [12] F. K. Guo, H. J. Jing, U. G. Meissner and S. Sakai, Phys. Rev. D **99**, 091501 (2019); arXiv:1903.11503 [hep-ph].
- [13] M. Z. Liu *et al.*, Phys. Rev. Lett. **122**, 242001 (2019); arXiv:1903.11560 [hep-ph].
- [14] J. R. Zhang, arXiv:1904.10711 [hep-ph].
- [15] H. Huang, J. He and J. Ping, arXiv:1904.00221 [hep-ph].
- [16] Y. Shimizu, Y. Yamaguchi and M. Harada, arXiv:1904.00587 [hep-ph].
- [17] C. W. Xiao, J. Nieves and E. Oset, Phys. Rev. D **100**, 014021 (2019); arXiv:1904.01296 [hep-ph].
- [18] L. Meng, B. Wang, G. J. Wang and S.-L. Zhu, Phys. Rev. D **100**, 014031 (2019) [arXiv:1905.04113 [hep-ph]]; J. B. Cheng and Y. R. Liu, Phys. Rev. D **100**, 054002 (2019) [arXiv:1905.08605 [hep-ph]].
- [19] J. J. Wu, R. Molina, E. Oset and B. S. Zou, Phys. Rev. Lett. **105**, 232001 (2010) [arXiv:1007.0573 [nucl-th]]; J. J. Wu, R. Molina, E. Oset and B. S. Zou, Phys. Rev. C **84**, 015202 (2011) [arXiv:1011.2399 [nucl-th]]; W. L. Wang, F. Huang, Z. Y. Zhang and B. S. Zou, Phys. Rev. C **84**, 015203 (2011) [arXiv:1101.0453 [nucl-th]]; J. J. Wu, T.-S. H. Lee and B. S. Zou, Phys. Rev. C **85**, 044002 (2012) [arXiv:1202.1036 [nucl-th]]; Z. C. Yang, Z. F. Sun, J. He, X. Liu and S.-L. Zhu, Chin. Phys. C **36**, 6 (2012) [arXiv:1105.2901 [hep-ph]]; C. Garcia-Recio, J. Nieves, O. Romanets, L. L. Salcedo and L. Tolos, Phys. Rev. D **87**, 074034 (2013) [arXiv:1302.6938 [hep-ph]]; Y. Huang, J. He, H. F. Zhang and X. R. Chen, J. Phys. G **41**, no.11, 115004 (2014) [arXiv:1305.4434 [nucl-th]].
- [20] T. Gutsche and V. E. Lyubovitskij, Phys. Rev. D **100**, 094031 (2019); arXiv:1910.03984 [hep-ph].
- [21] X.-Y. Wang, J. He and X. Chen, arXiv:1912.07156 [hep-ph].



- [22] A. Accardi *et al.*, Eur. Phys. J. A **52**, 268 (2016);  
arXiv:1212.1701 [nucl-ex].
- [23] M. Lomnitz and S. Klein, Phys. Rev. C **99**, 015203 (2019);  
arXiv:1803.06420 [nucl-ex].
- [24] X. Li *et al.*, arXiv:2002.05880 [nucl-ex].
- [25] X. Chen, "A Plan for Electron Ion Collider in China", PoS DIS **2018**, 170 (2018);  
arXiv:1809.00448 [nucl-ex].
- [26] X. Chen, "Electron–Ion Collider in China", PoS SPIN **2018**, 160 (2019).
- [27] A. Mishra and D. Pathak, Phys. Rev. C **90**, 025201 (2014);  
arXiv:1404.2517 [nucl-th].
- [28] S. V. Efremov and E. Ya. Paryev, Eur. Phys. J. A **1**, 99 (1998).
- [29] E. Ya. Paryev, Eur. Phys. J. A **7**, 127 (2000).
- [30] E. Ya. Paryev, Chinese Physics C, Vol. **42**, No. (8), 084101 (2018).
- [31] T. Song, K. C. Han and C. M. Ko, Phys. Rev. C **85**, 014902 (2012);  
arXiv:1109.6691 [nucl-th].
- [32] X. Du, M. He and R. Rapp, arXiv:1704.04838 [hep-ph].
- [33] X. Du, S. Liu and R. Rapp, arXiv:1904.00113 [nucl-th].
- [34] J. Breitweg *et al.* (ZEUS Collaboration), Phys. Lett. B **437**, 432 (1998);  
arXiv:hep-ex/9807020.
- [35] C. Adloff *et al.* (H1 Collaboration), Phys. Lett. B **483**, 23 (2000);  
arXiv:hep-ex/0003020.
- [36] S. Chekanov *et al.* (ZEUS Collaboration), Phys. Lett. B **680**, 4 (2009);  
arXiv:0903.4205 [hep-ex].
- [37] A. M. Sirunyan *et al.* (CMS Collaboration), Eur. Phys. J. C **79**, No.3, 277 (2019);  
arXiv:1809.11080 [hep-ex].
- [38] R. Aaij *et al.* (LHCb Collaboration), JHEP **1509**, 084 (2015);  
arXiv:1505.08139 [hep-ex].
- [39] Y. Hatta, M. Strikman, J. Xu, and F. Yuan, arXiv:1911.11706 [hep-ph].
- [40] S. J. Brodsky, E. Chudakov, P. Hoyer, J. M. Laget, Phys. Lett. B **498**, 23 (2001).
- [41] M. Karliner and J. L. Rosner, Phys. Lett. B **752**, 329 (2016);  
arXiv:1508.01496 [hep-ph].
- [42] J. J. Wu, L. Zhao and B. S. Zou, arXiv:1011.5743 [hep-ph].
- [43] C. W. Xiao and E. Oset, Eur. Phys. J. A **49**, 139 (2013);  
arXiv:1305.0786 [hep-ph].

- [44] H. Huang and J. Ping, Phys. Rev. D **99**, 014010 (2019);  
arXiv:1811.04260 [hep-ph].
- [45] J. Wu, Y. R. Liu, K. Chen, X. Liu and S.-L. Zhu, Phys. Rev. D **95**, 034002 (2017);  
arXiv:1701.03873 [hep-ph].
- [46] Y. Yamaguchi *et al.*, Phys. Rev. D **96**, 114031 (2017);  
arXiv:1709.00819 [hep-ph].
- [47] B. Wang, L. Meng and S. L. Zhu, JHEP **1911**, 108 (2019);  
arXiv:1909.13054 [hep-ph].
- [48] V. Kubarovsky and M. B. Voloshin, Phys. Rev. D **92**, 031502 (2015);  
arXiv:1508.00888 [hep-ph].
- [49] A. N. Hiller Blin *et al.*, Phys. Rev. D **94**, 034002 (2016).
- [50] S. Joosten and Z.-E. Meziani, arXiv:1802.02616 [hep-ex].